Eur. Phys. J. A (2015) **51**: 37
DOI 10.1140/epja/i2015-15037-8

THE EUROPEAN PHYSICAL JOURNAL A

Regular Article – Theoretical Physics

^{3}H/^{3}He ratio as a probe of the nuclear symmetry energy at sub-saturation densities

Yongjia Wang[1,2], Chenchen Guo[1,3], Qingfeng Li[1,a], and Hongfei Zhang[2]

[1] School of Science, Huzhou University, Huzhou 313000, P.R. China
[2] School of Nuclear Science and Technology, Lanzhou University, Lanzhou 730000, P.R. China
[3] College of Nuclear Science and Technology, Beijing Normal University, Beijing 100875, P.R. China

Received: 28 July 2014 / Revised: 8 December 2014
Published online: 26 March 2015 –
Communicated by A. Ramos

Abstract. Within the newly updated version of the ultra-relativistic quantum molecular dynamics (UrQMD) model in which the Skyrme potential energy-density functional is introduced, the yield ratio between ^{3}H and ^{3}He clusters emitted from central ^{40}Ca + ^{40}Ca, ^{96}Zr + ^{96}Zr, ^{96}Ru + ^{96}Ru, and ^{197}Au + ^{197}Au collisions in the beam energy range from 0.12 to 1 GeV/nucleon is studied. The recent FOPI data for the ^{3}H/^{3}He ratio are compared with UrQMD calculations using 13 Skyrme interactions (all exhibiting similar values of iso-scalar incompressibility but very different density dependences of the symmetry energy). It is found that the ^{3}H/^{3}He ratio is sensitive to the nuclear symmetry energy at sub-saturation densities. Model calculations with moderately soft to linear symmetry energies are in qualitatively agreement with the ^{3}H/^{3}He ratio data of the FOPI Collaboration. This result is in line with both the recent constraints on the low-density symmetry energy available in the literature and our previous results for the high-density symmetry energy obtained with the elliptic flow of free nucleons and hydrogen isotopes as a sensitive probe.

1 Introduction

The density dependence of the nuclear symmetry energy is a hot topic in both nuclear and astrophysics, due to its importance for the structure of exotic nuclei, the dynamics of heavy-ion collisions (HICs) induced by neutron-rich nuclei, and the properties of neutron stars and other astrophysical phenomena. It is also one of the important goals of the current and future rare isotope beam facilities (*e.g.* CSR at HIRFL, FAIR at GSI, SPIRAL2 at GANIL, FRIB at MSU, RIBF at RIKEN) around the world. For recent reviews see refs. [1–3].

The energy per nucleon of isospin asymmetric nuclear matter can be generally expressed as $e(\rho,\delta) = e_0(\rho,0) + e_{\rm sym}(\rho)\delta^2$, where $\delta = (\rho_n - \rho_p)/(\rho_n + \rho_p)$ is the isospin asymmetry, and ρ_n, ρ_p, and ρ are the neutron, proton and total nucleon densities. $e_0(\rho,0)$ is the energy per nucleon of the isospin symmetric nuclear matter, while $e_{\rm sym}(\rho)$ is the nuclear symmetry energy. Thanks to the continuing endeavor of both nuclear physicists and astrophysicists in recent years, many sensitive probes from nuclear structure, nuclear reactions and neutron stars have been used to estimate parameters (*e.g.*, the coefficient $S_0 = e_{\rm sym}(\rho_0)$ and the slope parameter $L = 3\rho_0\big(\frac{\partial e_{\rm sym}(\rho)}{\partial\rho}\big)\big|_{\rho=\rho_0}$) of the symmetry energy at saturation density (ρ_0). So far, the value of the nuclear symmetry energy at $\rho \approx 0.11\,{\rm fm}^{-3}$ has been relatively well constrained but its value at other densities or, generally, its density dependence has still large uncertainties (see, *e.g.*, refs. [4–10]).

The ratio of ^{3}H and ^{3}He yields emitted from HICs has been suggested as a sensitive probe of the nuclear symmetry energy within both the Boltzmann-Uehling-Uhlenbeck (BUU) type and the quantum molecular dynamics (QMD) type transport models [11–15], still with some puzzling inconsistency. For example, in refs. [14,15] two QMD-type model calculations showed that the yield of ^{3}H calculated with a soft symmetry energy is larger than that with a stiff one, while in refs. [11,12] the isospin-dependent BUU (IBUU) model calculations showed the opposite trend. In ref. [13], using the Gogny effective interaction (MDI) in the IBUU model, it was found that both, ^{3}H and ^{3}He yields, did not exhibit significant differences between the results for a soft and a stiff symmetry energy. Moreover, it was shown in ref. [16] that, using the IBUU04 model incorporated with a phase-space coalescence afterburner, the ^{3}H/^{3}He ratio was found not to be sensitive to the nuclear symmetry energy any more. Furthermore, a recent study in ref. [17] showed a large discrepancy regarding the ^{3}H/^{3}He ratio at low kinetic energies between Michigan State University experimental data and a BUU (often called pBUU) model as well as an improved QMD (often called ImQMD) model simulations, regardless of which parameterized symmetry energy is employed. Thus, in view

[a] e-mail: liqf@hutc.zj.cn

Table 1. Properties of nuclear matter at various densities as calculated by selected Skyrme parametrizations used in this work. All entries are in MeV, except for density in fm^{-3}.

					$\rho = 0.08$	$\rho = 0.055$	$\rho = 0.03$
	ρ_0	K_0	S_0	L	$e_{\mathrm{sym}}(\rho)$	$e_{\mathrm{sym}}(\rho)$	$e_{\mathrm{sym}}(\rho)$
Skz4	0.160	230.08	32.01	5.75	26.73	22.48	15.91
Skz2	0.160	230.07	32.01	16.81	24.90	20.30	13.82
SV-mas08	0.160	233.13	30.00	40.15	20.53	16.06	10.44
SLy4	0.160	229.91	32.00	45.94	22.17	17.68	11.89
MSL0	0.160	230.00	30.00	60.00	18.39	13.90	8.72
SkO'	0.160	222.36	31.95	68.94	19.12	14.36	8.97
SV-sym34	0.159	234.07	34.00	80.95	19.38	14.15	8.50
Rs	0.158	237.42	30.82	86.39	16.48	11.76	6.92
Gs	0.158	237.29	31.13	93.31	16.16	11.34	6.53
Ska35s25	0.158	241.30	36.98	98.89	20.39	14.73	8.78
SkI2	0.158	240.93	33.37	104.33	17.15	12.21	7.26
SkI5	0.156	255.79	36.64	129.33	17.75	12.34	7.22
SkI1	0.160	242.75	37.53	161.05	14.21	8.69	4.15

of the current status for the detection of both ^{3}H and ^{3}He clusters, the sensitivity of the nuclear symmetry energy to the ^{3}H/^{3}He ratio is a subject of continuing interest.

Recently, the large-acceptance apparatus FOPI at the Schwerionen-Synchrotron (SIS) at GSI has been used to collect a large amount of yield data for light charged particles (protons, ^{2}H, ^{3}H, ^{3}He, and ^{4}He) from intermediate energy HICs which has been made available in refs. [18,19]. This data set offers new opportunities for studying the ^{3}H/^{3}He ratio over wide ranges of both, beam energy and system size. Moreover, by using the updated Ultrarelativistic Quantum Molecular Dynamics (UrQMD) model in which the Skyrme potential energy-density functional is introduced, the newly measured flow data of light charged particles can be reproduced quite well [20,21]. In this version of the UrQMD model, the stiffness of the symmetry energy can be selected within a broad range by choosing different Skyrme interactions, rather than by varying the strength parameter γ in the potential term of the symmetry energy which, in addition, cannot be used to express a very soft symmetry energy [22]. In view of these developments, it seems timely to re-examine the sensitivity of the ^{3}H/^{3}He ratio to the symmetry energy and to see whether it can provide firm constraints on the stiffness of the density-dependent symmetry energy.

The paper is arranged as follows. In the next section the new version of UrQMD with the use of Skyrme potential energy density functionals and its key parametrizations are presented. In sect. 3, results for ^{3}H, ^{3}He and their ratio from HICs at SIS/GSI energies are shown and discussed. Finally, a summary is given in sect. 4.

2 Model description

The UrQMD model has been widely and successfully used to study nuclear reactions of $p + p$, $p + A$ and $A + A$ systems within a large range of beam energies, from low SIS/GSI up to the LHC/CERN [23–26]. In the present code, the nuclear effective interaction potential energy U is derived from the integration of the Skyrme potential energy density functional, $U_\rho = \int u_\rho \mathrm{d}^3 r$, and u_ρ reads

$$u_\rho = \frac{\alpha}{2}\frac{\rho^2}{\rho_0} + \frac{\beta}{\eta+1}\frac{\rho^{\eta+1}}{\rho_0^\eta} + \frac{g_{\mathrm{sur}}}{2\rho_0}(\nabla\rho)^2 + \frac{g_{\mathrm{sur,iso}}}{2\rho_0}[\nabla(\rho_n - \rho_p)]^2 + (A\rho^2 + B\rho^{\eta+1} + C\rho^{8/3})\delta^2 + g_{\rho\tau}\frac{\rho^{8/3}}{\rho_0^{5/3}}. \quad (1)$$

Here, α, β, η, g_{sur}, $g_{\mathrm{sur,iso}}$, A, B, C, and $g_{\rho\tau}$ are parameters which can be directly calculated using Skyrme parameters (see, *e.g.*, refs. [20,27]). In this work, we choose 13 Skyrme interactions Skz4, Skz2, SV-mas08, SLy4, MSL0, SkO', SV-sym34, Rs, Gs, Ska35s25, SkI2, SkI5, and SkI1 [28], which give quite similar values of the incompressibility K_0 but different L values (the saturation properties of the selected forces are shown in table 1). In addition, the symmetry energies at $\rho = 0.08$, 0.055, and $0.03\,\mathrm{fm}^{-3}$ are also shown in table 1.

Figure 1 shows the density dependence of the symmetry energy for Skyrme interactions Skz4, Skz2, SLy4, MSL0, SkO', SV-sym34, Ska35s25, Gs, and SkI1. For comparison, very recent constraints extracted from nuclear properties as, *e.g.*, binding energy, neutron skin thickness, and isovector giant quadrupole resonance [6–10], are also presented. The symmetry energy predicted by SLy4 lies quite close to the upper limit of the result obtained by Danielewicz *et al.* [6], and also covers the results obtained by Brown [9] and by Zhang and Chen [8]. The symmetry energy determined by Roca-Maza *et al.* [7] for the density $0.1\,\mathrm{fm}^{-3}$ is very close to the results predicted with SkO' as well as SV-sym34. Furthermore, the density dependent symmetry energies in MSL0, SkO', SV-sym34, and Ska35s25 are very close to each other at low densities (below $0.06\,\mathrm{fm}^{-3}$) but well separated at high densities.

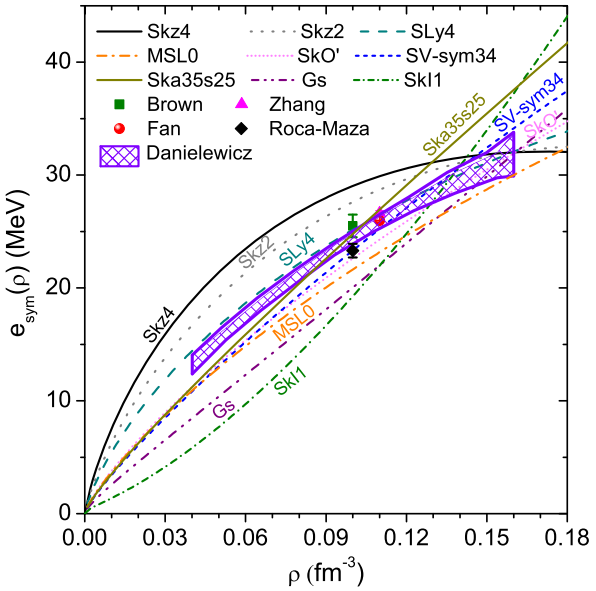

Fig. 1. (Color online) Density dependence of the symmetry energy for Skz4, Skz2, SLy4, MSL0, SkO', SV-sym34, Ska35s25, Gs, and SkI1. The shaded region exhibits the result obtained by Danielewicz *et al.* [6]. The four different scattered symbols represent recent constraints obtained by Roca-Maza *et al.* [7], Brown [9], Zhang *et al.* [8], and Fan *et al.* [10], as indicated.

The treatment of the collision term is the same as in our previous work in which the FP4 parametrization of the in-medium nucleon-nucleon cross section is employed [20]. Several ten thousand events of HICs are simulated in order to achieve small enough statistical uncertainties; error bars are hence not shown in the following figures, also for the sake of clarity. The simulation is stopped at 150 fm/c and an isospin-dependent minimum span tree algorithm (iso-MST) is used to construct clusters. Proton-proton or neutron-neutron (proton) pairs with relative distances smaller than $R_0^{pp} = 2.8$ fm or $R_0^{nn} = R_0^{np} = 3.8$ fm, respectively, and relative momenta smaller than $P_0 = 0.25$ GeV/c are considered to belong to the same cluster.

3 Results

Figure 2 illustrates the time evolution of the yields of ^{3}H (a), ^{3}He (b), and of their ratio ^{3}H/^{3}He (c) from Au + Au central ($b_0 < 0.15$) collisions at $E_{\rm lab} = 400$ MeV/nucleon. The reduced impact parameter b_0 is defined as $b_0 = b/b_{\rm max}$ with $b_{\rm max} = 1.15(A_P^{1/3} + A_T^{1/3})$. The Skz4, SkO', and SkI1 forces are chosen for this illustration as they correspond to the top, middle, and bottom curves at low densities among the cases shown in fig. 1. From fig. 2 it is, first of all, seen that most of the ^{3}H and ^{3}He clusters are produced within the time span from 30 fm/c to 60 fm/c. During this interval, the central nucleon density drops from normal to sub-normal (see, *e.g.*, fig. 2 in ref. [14] which shows that the high-density state is limited to the time span from about 5 fm/c to 30 fm/c for a similar colliding system).

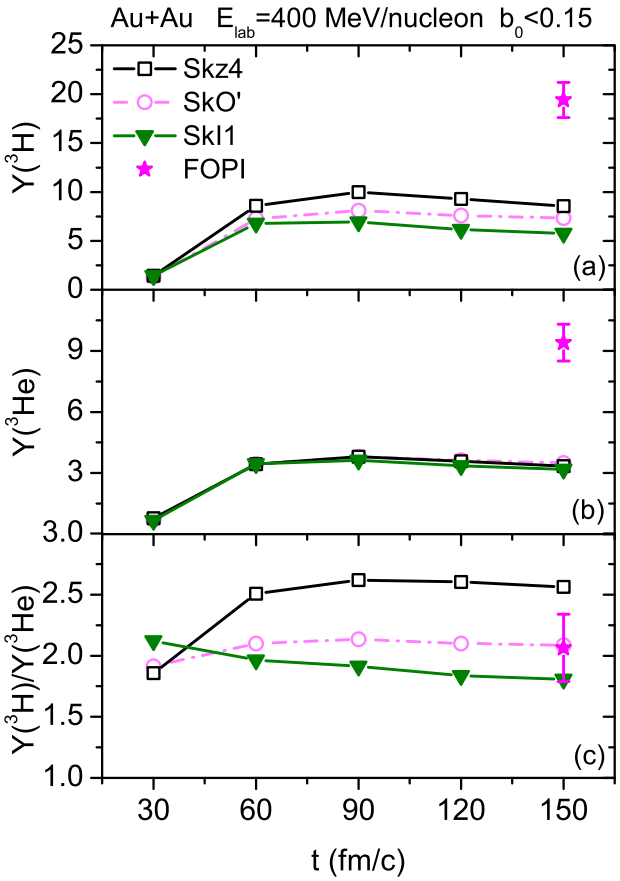

Fig. 2. (Color online) Time evolution of ^{3}H (in plot (a)) and ^{3}He (in (b)) yields and of their ratio ^{3}H/^{3}He (in (c)) from Au + Au collisions at $E_{\rm lab} = 400$ MeV/nucleon with centrality $b_0 < 0.15$. Calculations (lines with symbols) with Skz4, SkO', and SkI1 are compared with the 4π reconstructed FOPI data [18] (solid stars). It is noticed that the magnitude of experimental errors for the ^{3}H/^{3}He ratio is calculated using the propagation of errors, assuming the measurements of ^{3}H and ^{3}He yields are uncorrelated, while this assumption is not necessarily valid due to possible correlations in the detection system.

Secondly, the UrQMD model calculations underestimate the yields of both ^{3}H and ^{3}He. Due to the lack of some quantum features and without considering the antisymmetrized wave function in the QMD-like models, as well as our poor knowledge about the range and strength of the nuclear potential in a nuclear medium at finite temperature, this underestimation can not be resolved solely by considering uncertainties in the stiffness of the equation of state or in the medium modification of the two-body collision term. However, one sees that the ^{3}H yield is sensitive to the Skyrme interaction whereas the ^{3}He yield does not exhibit this sensitivity. As is evident from table 1, these Skyrme parametrizations are selected to have large differences only in the value of L. However, the emission of ^{3}H is affected by the nuclear symmetry potential, while the ^{3}He yield is also affected by the Coulomb potential between two protons which reduces the sensitivity to the symmetry energy, as discussed in refs. [29,30]. Finally, we see that the SkI1 parametrization results in the smallest

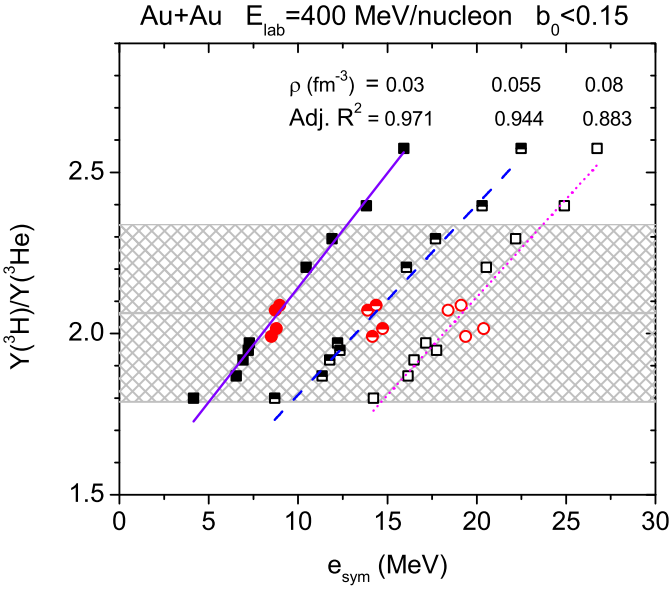

Fig. 3. (Color online) ^{3}H/^{3}He ratio as a function of symmetry energy at densities of $\rho = 0.08$ (open symbols), 0.055 (half-solid symbols), and 0.03 (solid symbols) fm^{-3}. Four circle symbols in each group denote calculations with MSL0, SkO', SV-sym34, and Ska35s25, and square symbols represent calculations with the other 9 Skyrme interactions listed in table 1. The lines represent linear fits to calculations for the three density cases. Correspondingly, the Adj. R^2 values are also given. The shaded region indicates the FOPI data of ^{3}H/^{3}He ratio [18].

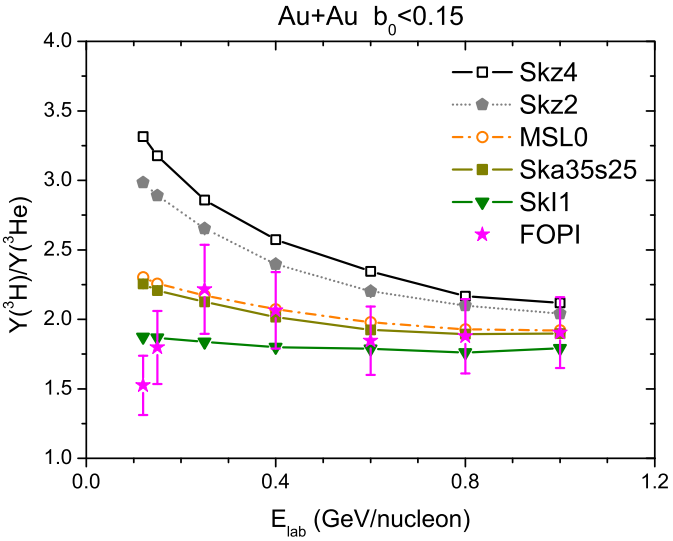

Fig. 4. (Color online) Excitation function of the ^{3}H/^{3}He ratio from central ($b_0 < 0.15$) Au + Au collisions. Calculations with Skz4, Skz2, MSL0, Ska35s25, and SkI1 are represented by different lines with symbols. The FOPI data (stars) are taken from ref. [18].

^{3}H yield, while Skz4 leads to the largest ^{3}H yield. This follows from the fact that, in a neutron-rich environment at sub-normal density, Skz4 gives a more repulsive symmetry potential, leading to a larger phase-space distribution for neutrons. Hence, more neutrons and neutron-rich light clusters such as ^{3}H are produced. Similar results were also obtained in two other QMD-type models [14,15].

If we turn to fig. 2(c), we observe that, during the initial stage at times $t < 40\,\mathrm{fm}/c$, the SkI1 force gives the larger ^{3}H/^{3}He ratio while, at the final stage, this is the case for Skz4. At $t < 40\,\mathrm{fm}/c$, ^{3}H and ^{3}He consist of protons and neutrons which evolve mainly from the supra-saturation density region and are emitted early; a stiff symmetry energy will thus cause more neutrons and less protons to be emitted than a soft one. More ^{3}H can be formed, resulting in a higher value of the ^{3}H/^{3}He ratio as well as of the ratio of free neutrons to protons. Very similar results can be found in other QMD-type model calculations [14,31,32]. As the reaction proceeds, the formed hot and dense system decompresses and more and more nucleons and light clusters will evolve and emerge from a low-density environment. The opposite effect of the symmetry energy on the ^{3}H/^{3}He ratio should appear. It follows that, at the asymptotic stage, the ^{3}H/^{3}He ratio predominantly reflects the symmetry energy at sub-saturation densities.

Figure 3 shows the ^{3}H/^{3}He ratios calculated with the 13 selected Skyrme parametrizations as a function of the symmetry energy at three sub-normal density points: 0.08, 0.055, and 0.03 fm^{-3}. The line in each bunch represents a linear fit to the calculations, the respective value of the adjusted coefficient of determination (Adj. R^2) is also shown. It can be seen that the linearity between the ^{3}H/^{3}He ratio and the symmetry energy increases with decreasing density, which indicates a strong correlation between them at low densities. (We also tested the linearity between the ratio and the slope parameter L, the value of Adj. R^2 is 0.804, indicating the ^{3}H/^{3}He ratio correlates strongly with the symmetry energy at low densities rather than its slope parameter L.) The ^{3}H/^{3}He ratios calculated with MSL0, SkO', SV-sym34, and Ska35s25 (which give almost the same value of the symmetry energy at $\rho = 0.03\,\mathrm{fm}^{-3}$, see table 1) are close to each other and centered in the shaded band, while the results obtained with Skz4 and Skz2 fall outside the band. Obviously, the large uncertainty of the experimental data prevents us from getting a tighter constraint on the density-dependent symmetry energy. Furthermore, it is noted [33,34] that different cluster recognition criteria affect the neutron/proton as well as ^{3}H/^{3}He ratios, especially at small kinetic energies. Therefore, the comparison of the full energy spectrum with the experimental data seems mandatory for a future study.

Luckily, the comparison to experimental ^{3}H/^{3}He data as functions of beam energy and system size and composition has become possible, supplying a more systematic and thus more consistent information on the symmetry energy. Figure 4 displays firstly the ^{3}H/^{3}He ratio as a function of beam energy. Calculations performed with Skz4, Skz2, MSL0, Ska35s25, and SkI1 are compared to the experimental data represented by the stars. At low beam energies (below 200 MeV/nucleon), the ratio is quite sensitive to the density dependence of the symmetry energy, however, the experimental data cannot be well reproduced. The disagreement of calculations with data implies again that the method for constructing clusters is not fully valid at low beam energies. Above 200 MeV/nucleon, the ratio

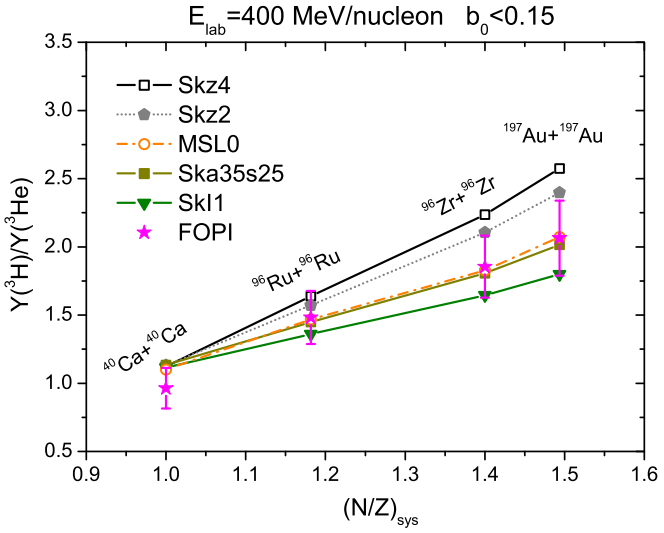

Fig. 5. (Color online) ^{3}H/^{3}He ratio from central ($b_0 < 0.15$) ^{40}Ca + ^{40}Ca, ^{96}Ru + ^{96}Ru, ^{96}Zr + ^{96}Zr, and ^{197}Au + ^{197}Au collisions at $E_{\rm lab} = 400$ MeV/nucleon as a function of neutron/proton ratio of the colliding system. The FOPI data (stars) are taken from ref. [18].

is still sensitive to the symmetry energy, but the sensitivity decreases with increasing beam energy due to the increase of both, the nucleon density and the number of nucleon-nucleon collisions. Furthermore, the calculations with MSL0 and Ska35s25, for which the difference in L is as large as ~ 39 MeV, are very close to each other, indicating the sensitivity of the ^{3}H/^{3}He ratio to the stiffness of the symmetry energy is more obvious at low densities.

Figure 5 displays the calculated ^{3}H/^{3}He ratios as a function of the neutron/proton ratio of the colliding systems in comparison with the FOPI data for central collisions at $E_{\rm lab} = 400$ MeV/nucleon. The reaction systems are ^{40}Ca + ^{40}Ca, ^{96}Ru + ^{96}Ru, ^{96}Zr + ^{96}Zr, and ^{197}Au + ^{197}Au. For the isospin symmetric ^{40}Ca + ^{40}Ca case, the results with the five selected Skyrme forces are very close to each other. With the increase of isospin asymmetry by varying systems from ^{96}Ru + ^{96}Ru to ^{197}Au + ^{197}Au, the calculated results are well separated due to an increasingly stronger effect of the symmetry energy at sub-normal densities. Especially, calculations using both MSL0 and Ska35s25 (as well as SkO' and SV-sym34, not shown in the figure), which represent a moderately soft to linear symmetry energy, reproduce the data fairly well. Although a desirable tighter constraint to the density dependence of the symmetry energy is still not achieved here, partly due to the large experimental uncertainties, a very satisfactory consistency among the presented comparisons is achieved.

4 Summary

Utilizing the recently updated UrQMD model in which the Skyrme potential energy density functional is adopted, we have studied the isospin pair ^{3}H and ^{3}He production in heavy-ion collisions at intermediate energies. The ^{3}H/^{3}He yield ratio is shown to exhibit a large sensitivity to the nuclear symmetry energy at sub-saturation densities. This result is similar to most previous studies using BUU-type and QMD-type transport models, but differences in the influence of the symmetry energy on the yield of (and ratio between) light clusters are also observed between these model calculations, which certainly requires further investigations.

In the current work, simulations with 13 selected Skyrme interactions are compared with the recent FOPI data. It is found that those calculations for the dependence on the nucleon-density, beam energy, and system size and composition of the ^{3}H/^{3}He ratio employing MSL0, SkO', SV-sym34, and Ska35s25 (which parameterize a moderately soft to linear symmetry energy) are all in good semi-quantitative agreement with FOPI data. Calculations using Skz4 and Skz2 which parameterize a very soft symmetry energy are far from the data. It is observed that the current extraction of the stiffness of the symmetry energy at sub-normal densities with the ^{3}H/^{3}He ratio as a probe is in line with previous studies for the low-density symmetry energy. It is more exciting that this result is also consistent with previous results based on the elliptic flow of free nucleons (and hydrogen isotopes) as a probe [21,35,36] which mainly provide information on the symmetry energy at supra-normal densities. However, additional calculations with other clustering algorithms and model assumptions will be certainly required to confirm the sensitivity of the ^{3}H/^{3}He ratio to the stiffness of the symmetry energy and the constraint obtained from this observable.

We thank Professor W. Trautmann for a careful reading of the manuscript. We acknowledge support by the computing server C3S2 in Huzhou University. The work is supported in part by the National Natural Science Foundation of China under Grants Nos. 11175074, 11405054 and 11375062, and the project sponsored by SRF for ROCS, SEM.

References

1. B.-A. Li, L.-W. Chen, C.M. Ko, Phys. Rep. **464**, 113 (2008).
2. C.J. Horowitz *et al.*, J. Phys. G: Nucl. Part. Phys. **41**, 093001 (2014).
3. B.-A. Li, A. Ramos, G. Verde, I. Vidana, Eur. Phys. J. A **50**, 9 (2014).
4. M.B. Tsang *et al.*, Phys. Rev. C **86**, 015803 (2012).
5. J.M. Lattimer, Y. Lim, Astrophys. J. **771**, 51 (2013).
6. P. Danielewicz, J. Lee, Nucl. Phys. A **922**, 1 (2014).
7. X. Roca-Maza *et al.*, Phys. Rev. C **87**, 034301 (2013).
8. Z. Zhang, L.-W. Chen, Phys. Lett. B **726**, 234 (2013).
9. B.A. Brown, Phys. Rev. Lett. **111**, 232502 (2013).
10. X. Fan, J. Dong, W. Zuo, Phys. Rev. C **89**, 017305 (2014).
11. L.-W. Chen, C.M. Ko, B.-A. Li, Phys. Rev. C **68**, 017601 (2003).
12. L.-W. Chen, C.M. Ko, B.-A. Li, Nucl. Phys. A **729**, 809 (2003).

13. L.-W. Chen, C.M. Ko, B.-A. Li, Phys. Rev. C **69**, 054606 (2004).
14. Q. Li, Z. Li, S. Soff, M. Bleicher, H. Stöcker, Phys. Rev. C **72**, 034613 (2005).
15. Y. Zhang, Z. Li, Phys. Rev. C **71**, 024604 (2005).
16. G.-C. Yong, B.-A. Li, L.-W. Chen, X.-C. Zhang, Phys. Rev. C **80**, 044608 (2009).
17. M. Youngs, PhD Thesis, Michigan State University (2013).
18. FOPI Collaboration (W. Reisdorf *et al.*), Nucl. Phys. A **848**, 366 (2010).
19. FOPI Collaboration (W. Reisdorf *et al.*), Nucl. Phys. A **876**, 1 (2012).
20. Y. Wang, C. Guo, Q. Li, H. Zhang, Z. Li, W. Trautmann, Phys. Rev. C **89**, 034606 (2014).
21. Y. Wang, C. Guo, Q. Li, H. Zhang, Y. Leifels, W. Trautmann, Phys. Rev. C **89**, 044603 (2014).
22. J. Dong, W. Zuo, J. Gu, U. Lombardo, Phys. Rev. C **85**, 034308 (2012).
23. Q. Li, C. Shen, C. Guo, Y. Wang, Z. Li, J. Lukasik, W. Trautmann, Phys. Rev. C **83**, 044617 (2011).
24. UrQMD-Collaboration (S.A. Bass *et al.*), Prog. Part. Nucl. Phys. **41**, 255 (1998).
25. M. Bleicher *et al.*, J. Phys. G **25**, 1859 (1999).
26. Q. Li, G. Graf, M. Bleicher, Phys. Rev. C **85**, 034908 (2012).
27. Y. Zhang, Z. Li, Phys. Rev. C **74**, 014602 (2006).
28. M. Dutra, O. Lourenco, J.S. Sa Martins, A. Delfino, J.R. Stone, P.D. Stevenson, Phys. Rev. C **85**, 035201 (2012) and M. Dutra, PhD Thesis, Universidade Federal Fluminense (2011).
29. C. Guo, Y. Wang, Q. Li, W. Trautmann, L. Liu, L. Wu, Sci. China Phys. Mech. Astron. **55**, 252 (2012).
30. Y. Wang, C. Guo, Q. Li *et al.*, Sci. China Phys. Mech. Astron. **55**, 2407 (2012).
31. S. Kumar, Y.G. Ma, G.Q. Zhang, C.L. Zhou, Phys. Rev. C **85**, 024620 (2012).
32. S. Kumar, Y.G. Ma, Phys. Rev. C **86**, 051601 (2012).
33. Q. Li, Mod. Phys. Lett. A **24**, 41 (2009).
34. Y. Zhang, Z. Li, C. Zhou, M.B. Tsang, Phys. Rev. C **85**, 051602 (2012).
35. P. Russotto, P.Z. Wu, M. Zoric, M. Chartier, Y. Leifels, R.C. Lemmon, Q. Li, J. Lukasik *et al.*, Phys. Lett. B **697**, 471 (2011).
36. M.D. Cozma, Y. Leifels, W. Trautmann, Q. Li, P. Russotto, Phys. Rev. C **88**, 044912 (2013).